Visualization of Intracardiac Atrial Electrograms of Patients with Atrial Fibrillation using Spectral Analysis

João Loures Salinet Jr., Guilherme N. Oliveira, Frederique Jos Vanheusden,
João Luiz Dihl Comba, Ghulam André Ng, Fernando Soares Schlindwein

Abstract—Atrial fibrillation is the most common cardiac arrhythmia, and it is associated with increased risk of stroke, heart failure and mortality. In this work we describe spectral analysis techniques that are being used in conjunction with visualization algorithms to help guide catheter ablation procedures that aim at treating patients with the arrhythmia.

Atrial Fibrillation (AF) is a serious problem as it can lead to stroke and heart failure, with increased mortality. To further complicate the problem, the precise electrical mechanisms underlying AF are not well understood. One effective treatment for AF is catheter ablation, whereby areas in the atria and/or nearby locations are targeted and ablated (or "burned"). However, results are variable, with a large number of patients requiring repeated procedures if AF recurs in the short term. Long term results are even less encouraging. One of the main issues with ablation is the decision on where to ablate that gives the maximum efficacy and safety. Improving understanding of the precise electrical mechanisms underlying AF is key to minimising the amount of "burning" with ablation and maximizing the gain. It is important that information is available to aid ablation decision and strategy either before or during the ablation procedure. Hence, techniques and technologies to characterize and map candidate locations for ablation need to be implemented in real-time. In this paper we describe a technique for mapping the dominant frequency (DF) of atrial electrograms and explore, implement and measure the processing time for several approaches for its implementation. Our solution leverages the parallel processing computation offered by multiple CPU cores, but more importantly, the massive parallel computational power available in current Graphic Processing Units (GPUs). We also describe techniques for visualizing the behavior of dominant frequency of intracardiac atrial electrograms. The visualization allows the mapping of the DFs using a color scale and isolating the main DF areas. We conclude that, with current technology and using an off-the-shelf, modern personal computer with a graphics card and costing about US$ 1,000 it is possible to implement real time DF mapping with a loading as low as 6.75% (up to 50% depending of the implementation strategy and the level of detail required). This changes the perspective of the problem from pure, basic research to translational, applied research and we propose an exciting new step forward in this important area.

Atrial Fibrillation

Measuring and modeling the genesis and propagation of the electrical activity in the heart in quantitative terms is a very important area of research that will help understand and treat heart arrhythmias. Atrial fibrillation (AF) is a heart rhythm disturbance characterized by uncoordinated and rapid electrical atrial activation which takes over from normal sinus rhythm, with consequent deterioration of the mechanical ability of the atria to pump blood effectively. The ventricles will beat irregularly and rapidly during AF when conduction is intact. On the ECG, the wave of depolarization that spreads throughout the atria, called P waves, are replaced by rapid, small amplitude oscillations which vary in amplitude, shape, and timing between QRS complexes (Fuster *et al*.[7]), which corresponds to the three graphical deflections (Q, R and S waves) seen on a typical electrocardiogram

Atrial Fibrillation is the most common cardiac arrhythmia encountered in clinical practice with a prevalence of 1-2% of the general population [4]. The symptoms of AF include palpitations, tiredness, shortness of breath, dizziness and chest pain. As the mechanical pumping ability of the atria is compromised, the resulting pooling of blood in the atria increases the long-term risk of stroke fivefold [6]. AF is a public health problem with approximately €3,700/year per patient being spent in Europe [7]. The cost of a catheter-based ablation procedure is about €12,500. Any advances in the understanding of this condition, especially advances that might lead to more effective treatment are, therefore, of great importance.

An affordable and recently popular approach is to take advantage of the computational power of graphic processing units (GPUs) to speed-up scientific computational codes. The parallel processing of GPUs, with hundreds of cores, allow considerable performance speed-ups. In this work we use GPUs to implement realistic models of electrical activity in cardiac muscle. We implemented a multi-channel signal analysis approach, which computes and display results over the 3D surface of the heart chamber under study in real time.

Dominant Frequency in Atrial Fibrillation

In 1913 Mines, in an elegant paper [13], studied the vulnerability of an excitable circle of cells in the heart. It follows from that original idea that if the concept of *reentry* is to be applied to atrial fibrillation, there would be a preferred range of *dominant frequencies* associated with the circuits. The problem is simply explained using the diagram in Figure 1. If reentry circuits are formed, knowing the velocity of propagation of the electrical activation (typically slower than 20 cms^{-1}), the size of the atrium (up to 6 cm) and, most importantly, the duration of the refractory period (about 200-240 ms in normal cardiac cells, but reduced down to about 80-85 ms in AF [3] then the DF range associated with AF would be between 4.2 Hz and 12.5 Hz.

Figure 1 also helps understand why small hearts (such as a rat's heart) are less capable of sustained fibrillation: a certain minimum critical mass is required for reentry circuits, otherwise the excitation wavefront will hit refractory tissues when they get back to the origin.

We have been measuring and characterizing the behaviour of DF in persistent atrial fibrillation (persAF) for the last 3 years using up to 2048 channels of atrial electrogram signals collected at 1200 Hz using a non-contact mapping system (EnSite^{TM} Array, St Jude Medical) (Ahmad *et al*.[2, 1], Nicolson *et al*.[14], Salinet Jr *et al*. [15, 17, 16, 18]) and performing analysis of the electrical activation in the frequency domain. The spectral analysis of all the 2048 channels needs to be implemented in real time, if such analysis is to be used as a tool (which would be complementary to the current time domain-based approaches) to help decide where to ablate. This approach needs to include the identification and characterization of the

- *João Loures Salinet Jr., Frederique J. Vanheusden and Fernando S. Schlindwein are with the Department of Engineering, University of Leicester, UK, e-mail: jl279,fjv2,fss1@leicester.ac.uk*
- *Guilherme N. Oliveira and João L.D. Comba are with the Instituto de Informática, Universidade Federal do Rio Grande do Sul, Brazil. e-mail: gnoliveira,comba@inf.ufrgs.br*
- *Ghulam André Ng is with the Department of Cardiovascular Science, University of Leicester, UK, e-mail: gan1@leicester.ac.uk*

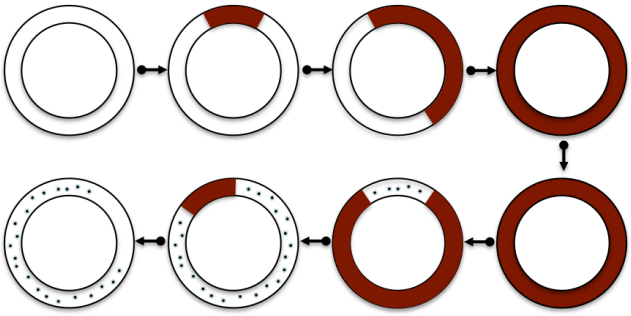

(a) Normal rhythm cycle excitation

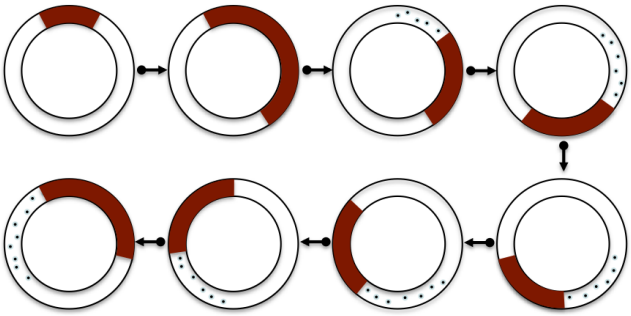

(b) Shorter refractory period and/or slower conduction

Figure 1. Schematic drawing for the normal rhythm cycle excitation (a) and an arrhythmic cycle excitation (b): excited state is represented in red and refractory state as dotted areas. In (a) the recirculation cannot occur, as when the stimulation completes a cycle the cells at that point are still refractory and cannot re-trigger. In (b), re-triggering can occur with either a shorter refractory period and/or slower conduction, allowing the development of a circulating wave. Modified from Mines [13].

DF in each of the 2048 spectral estimations, followed by a 3D representation on a screen in such a way that the clinician can manipulate (including rotate) the 3D maps representing the DF values. In this paper we explore (i) visualization techniques that help characterize the dominant frequency and (ii) different ways of using current technology to implement the spectral analysis and 3D mapping. The tools are based on the representation of the DF as color maps onto a 3D anatomically accurate representation of the atrium (figures 4, 5, 6 and 7). The alternatives explored and described in this paper to implement the signal processing were (i) using a single Pentium core under 64-bit Matlab; (ii) using multiple Pentium cores under 64-bit Matlab and its Parallel Toolbox, and (iii) using 480 GPU processors on a NVidia's GeForce GTX 570 card in C++ prototype.

Material and Methods

In recent years, a non-contact multi-electrode array catheter (St. Jude Medical, EnSite^{TM} Array) has been developed (Chinitz and Sethi[5], Kumagai and Nakashima[12], Tai and Chen[20]) to assist with the mapping of intracardiac electrical signals in complex arrhythmia cases. This innovation allows re-creation of a 3-dimensional (3D) geometry of the heart chamber(s) and the recorded electrical activity can be projected onto the geometry of the endocardial surface of the heart as simultaneous high density of virtual unipolar electrograms.

The balloon-mounted catheter with 64 electrodes arranged in an array fashion is placed within the blood pool of the cavity of interest and the electrograms from the endocardial surface of the chamber are collected using inverse solution mathematics and interpolation in an *inside-out* fashion. Up to 3600 points of electrical signals can be reconstructed by the EnSite 3000^{TM} system mapped onto the 3D representation of the atrium (Figure 2). For the off-line analysis the EnSite 3000^{TM} system can export up to 7s segments of data with up to 2048 points (a matrix of 32x64 spatial points) along the geometric coordi-

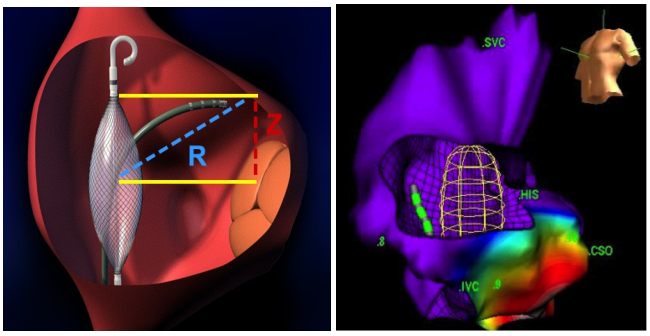

Figure 2. The ablation catheter and the EnSite 3000^{TM} balloon array are first used to map the inner surface of the heart's chamber using the ablation catheter as a probe and the balloon as reference. Then the array collects atrial electrograms (potentials) at 1200 Hz. The system can display the potentials as a color map. EnSite Array^{TM}and EnSite^{TM}are trademarks of St. Jude Medical, Inc. or its related companies. Reprinted with permission of St. Jude Medical^{TM}©2012. All rights reserved.

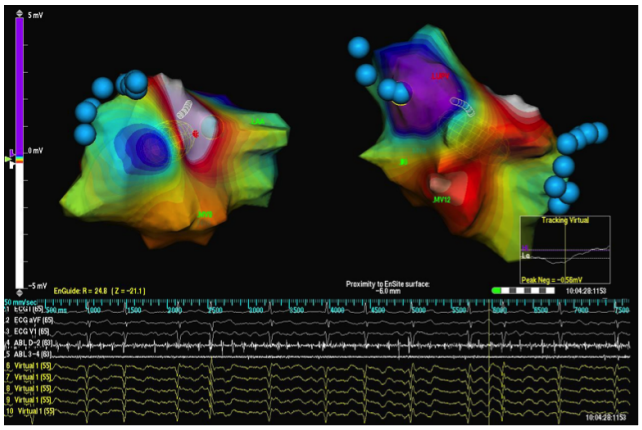

Figure 3. The activation voltage images (in the time domain) produced using the EnSite 3000^{TM} array. Two different views are presented simultaneously and can be independently re-oriented by the clinician performing the electrophysiological study (in theatre) followed by the ablation.

nates (x, y, z) of the shape of the atrium. The balloon was not moved after geometry creation, to avoid distortion of the signals and isopotential maps (Schilling *et al.*[19], Gornick *et al.*[9], Kadish *et al.*[11], Jais *et al.*[10]). Atrial unipolar electrograms were sampled at 1200 Hz and a high-pass filter embedded in the system with a cut-off frequency of 1 Hz was applied. No further filtering was applied to the electrogram signals to preserve their low frequency components[8]. We have exported several such segments and carefully merged them to compose longer data segments of 1 min duration for each patient for the studies described in this paper.

After data collection, the clinical EP mapping procedure was followed by ablation around the 4 pulmonary veins ostia aiming at electrical isolation of potential firing triggers localized in the pulmonary veins from the left atrium (Jais *et al.* 1997). This was performed either using point-by-point ablation guided by EnSite NavX or with a multielectrode pulmonary vein ablation catheter (PVAC, Medtronic Inc.) aimed at electrical isolation of conduction between the left atrium and pulmonary veins, which are important locations for firing triggers that initiate and perpetuate AF (Jais *et al.* 1997). This study was performed with informed consent from the patients undergoing AF ablation for the use of electrical data acquired.

Dominant Frequency Visualization using Spectral Analysis

For further investigation, the tool allows clinicians to isolate the highest DF area believed to be a key point on the maintenance of this ar-

rhythmia and track this area along time as illustrated in Figure 6. With current state-of-the art bedside equipment cardiologists who perform catheterization and ablation of AF use and manipulate 3D representations of the time domain analysis of the electrical activation (voltages) of any part of the heart. Figure 3 shows the visualization within the commercial system of non-contact intra-cardiac mapping using the intracardiac balloon technology of the EnSite^{TM} array.

We used a Fourier-based spectral analysis of the atrial electrograms for studying the behavior of the 3D dominant frequency maps, and determination of DF at each of the 2048 points given by the EnSite 3000^{TM} system. Figure 4 illustrates the whole spectral analysis procedure for each individual spatial point, the identification of the dominant frequency and color coding according to the frequency of the DF for the 3D representation of the DFs, with purple-blue representing the lower frequencies and red-dark red corresponding to higher frequencies. DF at each of the 2048 points was defined as the frequency with highest amplitude within the physiological relevant range (4 Hz to 12 Hz).

In Fourier-based spectral analysis, when N points of a signal $x(t)$ are sampled at frequency f_{sam} and their FFT is obtained, the time samples are at $T = 1/f_{sam}$ apart in the time domain and the resulting frequency samples are at $\Delta f = 1/NT$ apart in the frequency domain. In our case the original signals are sampled at f_{sam} = 1200 Hz and using 4s segments, and therefore $N = 4800$ points, $T = 1/1200(0.833ms)$ and $\Delta f = 0.25$ Hz. The original sequence of samples of $x(t)$ can be augmented with extra samples with zero amplitude to create longer sequences with, say $2N$ values (N original values of $x(t)$ augmented with N zeroes) or $5N$ values (N original values and $4N$ zeroes) before the FFT. This process is referred to as zero-padding. Although the spectral resolution does not improve with zero-padding, the resulting spectral estimations will have a finer representation in the frequency domain at $k/2NT$ or $k/5NT$, where the extra values are interpolations of the original $X(k/NT)$ and the interpolator is a $sin(f)/f$ kernel, producing the smoothest series that contains the original samples. In our case, when zero-padding factor is 2 the resulting frequency samples will be at $\Delta f_2 = 0.125$Hz and for zero-padding factor of 5, $\Delta f_5 = 0.05$Hz.

We have chosen to use 4-second long segments for a good compromise between frequency and time resolution, with a Hamming antileakage window. Consecutive DF maps were obtained 2s apart (with 50% overlap) after cancellation of the ventricular far field (QRS-T segments) on each of the 2048 unipolar atrial electrograms using an algorithm previously described [18]. A 3D DF frame of the left atrium is then generated using the anatomic coordinates exported and an example is displayed in Figure 5(a) with two different viewpoints. Figure 5(b) shows a time sequence of four consecutive frames which are 2s apart highlighting that the DF activity is dynamic.

With the advances in computing power and possibility of implementing more demanding mathematical manipulations of complex data and ability for producing and manipulating 3D imaging in real time as described here it is now possible to implement a system that measures the DF over say 2048 points and produces a 3D representation of the DF map in real time just as easily as the time domain voltage maps of figure 3 which are currently used to guide ablation. In figure 6 we illustrate how the visualisation of only the dominant frequency region can help doctors to identify the potential locations where ablation might take place. For this purpose, our tool needs to both identify the areas of highest DF, as well as use specific color-scales in the visualisation to clearly identify these areas.

Our tool also allows monitoring the impact of the ablation procedure in the frequency domain by comparing the 3D DF maps before and after ablation. This helps verify the effectiveness of the procedure. Figure 7 shows that a substantial reduction of both the DF frequency and the areas with high frequency occur after a successful ablation procedure. The lower part of Figure 7 shows the DF maps reproduced on the flat 32x64 matrix while the top part shows them as a more useful 3D representation taking the atrial geometry into consideration.

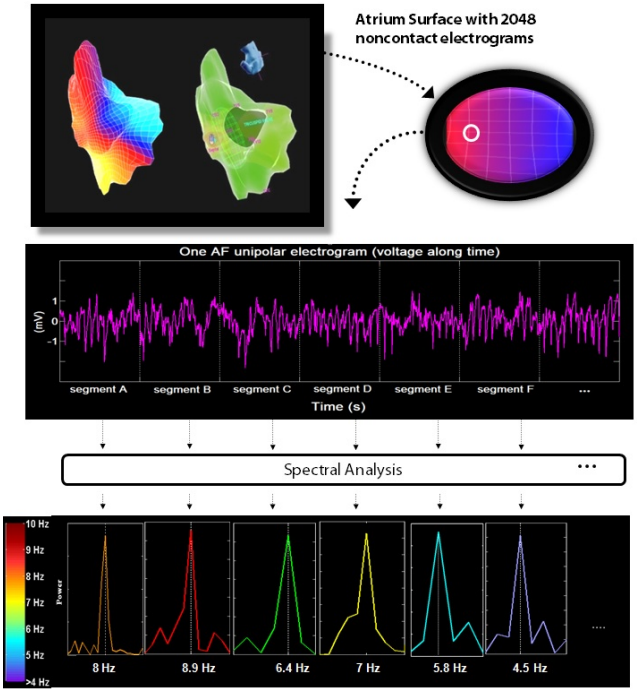

Figure 4. Spectral Analysis of the Dominant Frequency. The data collected by the EnSite 3000^{TM} System allows manipulation of the atrium on the screen and displays next to it the orientation of the torso. For each of the 2048 points of the 3D surface we obtain the dominant frequency (DF) of the atrial electrogram for each segment along time and then color-code the surface according to the frequency of the DF.

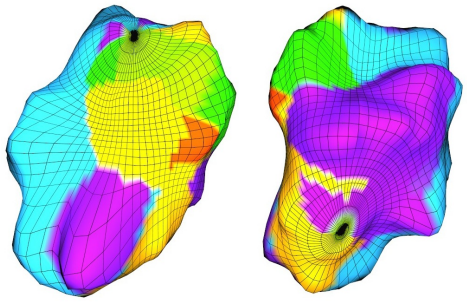

(a) views of the 3D DF mapping of the left atrium (LA)

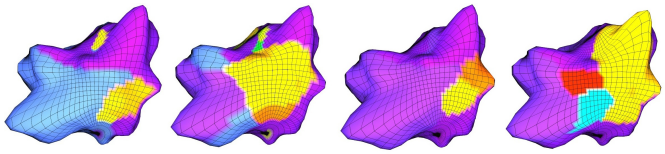

(b) sequence of four consecutive 3D DF mapping frames

Figure 5. 3D DF mapping of the left atrium. (a) two different views of the 3D DF mapping, and (b) a sequence of four consecutive 3D DF mapping frames which are 2 s apart for each representation.

Parallel Processing Implementations

DF maps were created with the Matlab 64-bit R2012a software and its corresponding Parallel Processing Toolbox (version 6.0). This software allows processing in double precision. The GPU implementation powered a C++ prototype, that created each DF map by computing the 2048 FFTs in parallel in the GPUs with the NVIDIA®CUDA^{TM}Fast Fourier Transform library (CUFFT), and later, identifying the frequency with highest amplitude for each FFT result, also in parallel, but

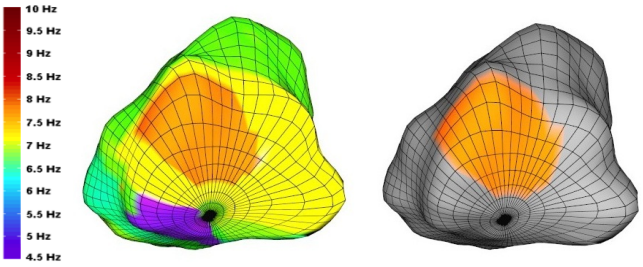

(a) (b)

Figure 6. 3D DF mapping and highest DF identification. (a) The 3D representation of the left atrium including the mapping of the dominant frequencies, DF (represented in a color scale) will help doctors visualize the behavior of the electrical activation of the atrium in the frequency domain in real time. The system can also automatically identify the region corresponding to the highest DF area (b).

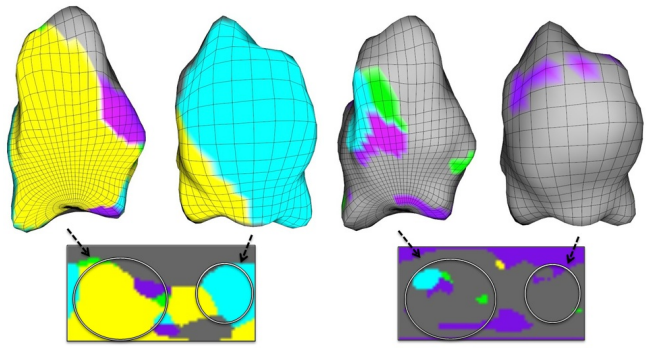

(a) baseline DF (b) DF after the PVI procedure

Figure 7. 3D DF mapping of the left atrium of a patient with persistent AF. In (a) we show the baseline DF map and in (b) the DF immediately after the standard Pulmonary Veins Isolation (PVI) procedure. The figure demonstrates a general reduction of the size of the DF areas, a reduction of the dominant frequency values and a reduction in the complexity of the DF areas after the PVI procedure.

now using CPU threads with OpenMP. Even though CUFFT library allows double precision computation, FFT calculations were done with single precision to reduce time spend sending the input data to GPU memory and the output data back to RAM. Also, using double precision, depending on the window size, can require more memory than the graphics card has available and so the computation of the 2048 FFTs would have to be divided in multiple smaller batches. With single precision 2048 FFTs could be computed in a single batch, which means a single pair of input-in and output-out data transfer and faster computation. Aware that this could possibly decrease precision and lead to errors, we evaluated the difference between the single precision GPU computed FFT results and the double precision MATLAB ones, and found the average mean squared error values to be negligible when compared to the RMS level of the resulting signal.

Results

A 3.4 GHz Pentium i7 quad core desktop was used to determine the processing time for DF-mapping with different number of CPU cores. For comparison of processing times between single and multiple CPU cores and the GPU cores, a 1 minute data segment was analysed using 4s windows with 50% overlap. The zero-padding factor was set to 2 for allowing the visualization of frequency powers at every 0.125 Hz. Using a single CPU core (under Matlab), DF maps could be generated within 2.46$\pm$0.05 seconds. The processing time decreases to 2.03$\pm$0.03 seconds when using 4 Pentium cores (under Matlab). This means that the loading is about 50%. A real-time DF mapping implementation would therefore be possible by using just the CPU (Pentium) cores. Using the GPUs for FFT calculation decreases processing time to 0.27 $\pm$ 0.01 s. This is 14.8 times faster than real time (a load of only 6.75%). Even when the zero padding factor was increased to 5 (allowing visualization of frequency powers at every 0.05 Hz), the data processing using the GPUs under C++ was still 3.5 times faster than using 4 CPU cores under Matlab. These results therefore suggest that, where possible, using GPU cores for independent calculations on large amount of data is preferable. This would allow the use of the CPU Pentium cores to run other tasks concurrently, e.g. controlling data acquisition and storage. The timings considering different choices of zero-padding and the different approaches are shown in figure 8.

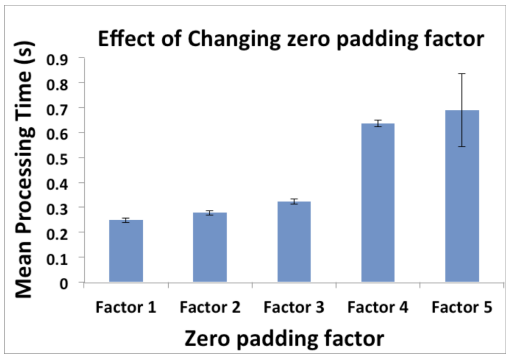

(a)

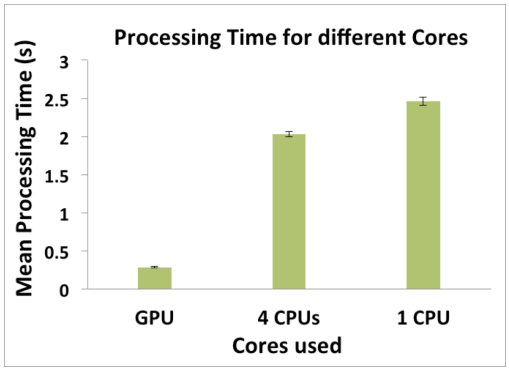

(b)

Figure 8. (a) Estimated processing time for different factors of zero-padding and (b) comparison of processing times between single and multiple CPU cores and the GPU cores for a factor-2 zero-padding.

The C++ visualisation displays the 3D DF like in electrograms, with the difference that each vertex color represents the dominant frequency instead of the electric potential. The fast rendering allows the user to perform rotation on the atrium surface, and the use of an interactive color scale that can be modified at any time to help visually isolate regions where the DFs are above a given threshold.

Leveraging the speed up obtained in the creation of the 3D DFs resulting from the use of GPUs, we also added two parameters that can be changed to make a trade-off between processing time and smoothness in consecutive DF maps: the zero-padding factor, and the percentage of overlapping between input signal windows. Increasing the zero-padding factor will lead to a finer representation of the resulting frequencies of the FFTs, and also higher memory requirement, as well as processing time (as shown in figure 8). When windows overlap, more DFs are created, thus reducing the time difference between consecutive ones. The result is a smoother animation of the DF maps, which helps to track the movement of the several frequency zones in the atrium. An example of such smooth animation is shown in figure 9, where the window length was 4 seconds, with a overlapping of 92%. The same configuration but with overlapping of half window, would display only the first and sixth frames.

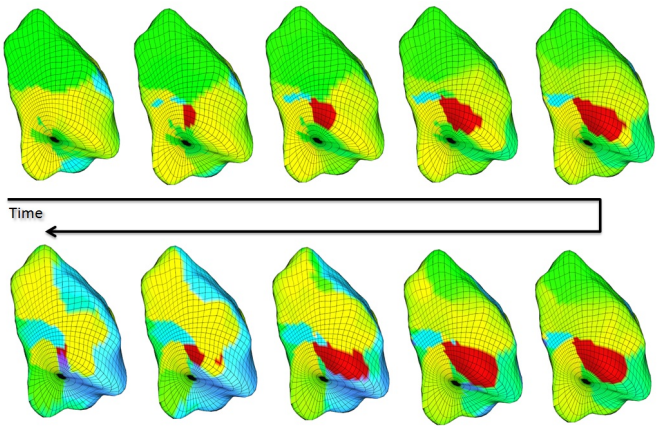

Figure 9. Consecutive DF maps using 92% of overlapping between windows: Using more overlapping creates more frames and a smoother animation that helps to understand how the different DF zones evolve over the surface along time.

Conclusions

The approaches described in this paper allow the same current state-of-the art bedside equipment used by clinicians nowadays to be easily modified to perform frequency domain analysis of the electrical activation of any chamber of the heart and generation of DF maps in real time. These 3D representations can be displayed with the same equipment and manipulated in exactly the same way as cardiologists who perform the catheterization and ablation procedures are used for manipulating the time-domain based images. With current technology and using a standard off-the-shelf PC with a modern graphics card, all of the approaches described here can be implemented in real time and can help the cardiologist performing ablation in the theatre by displaying frequency domain-based information in real time. Clearly using GPUs represents a tremendous advance, as the CPU cores can perform other jobs, such as the control of data acquisition and data transfer, or even be used to display the results in more informative ways.

Furthermore, we would like to stress the importance of having research groups with different expertise in this project. The use of scientific visualisation techniques and parallel programming using GPUs to this clinical project allowed us to develop a solution that is not currently available in real time with any existing equipment. We are currently exploring other avenues on how this prolific collaboration can continue to this and other clinical projects, and hope this work can serve as an example of other collaborations in interdisciplinary fields.

Acknowledgements

J.L. Salinet Jr, G.N. Oliveira and J.L.D. Comba wish to acknowledge CNPq (Processes 200598/2009-0, 140983/2011-2, 309483/2011-5 and 476685/2012-5). This study is part of the research portfolio supported by the National Institute for Health Research Leicester Cardiovascular Biomedical Research Unit and F.S. Schlindwein, G.A. Ng and F.J. Vanheusden wish to acknowledge funding from NIHR Leicester Cardiovascular BRU. F.S. Schlindwein wishes to acknowledge the receipt of a Santander Travel Grant that allowed him to visit UFRGS in Porto Alegre, Brazil, to get the research on GPU implementation started.

References

[1] A. Ahmad, J. Salinet, P. Brown, J. Tuan, P. Stafford, G. Ng, and F. Schlindwein. QRS subtraction for atrial electrograms: flat, linear and spline interpolations. *Medical and Biological Engineering and Computing*, 49:1321–1328, 2011. 10.1007/s11517-011-0829-9.

[2] A. Ahmad, F. S. Schlindwein, and G. A. Ng. Comparison of computation time for estimation of dominant frequency of atrial electrograms: Fast Fourier Transform, Blackman Tukey, Autoregressive and Multiple Signal Classification. *Journal of Biomedical Science and Engineering*, 3(9):843–847, 2010.

[3] V. Biktashev. *Computational Biology of the Heart*, chapter Control of re-entrant vortices by electrical stimulation, pages 137–170. John Wiley and Sons (editors A. V. Panfilov and A. V. Holden), 1997.

[4] A. Bollmann and F. Lombardi. Electrocardiology of atrial fibrillation. *Engineering in Medicine and Biology Magazine, IEEE*, 25(6):15 –23, nov.-dec. 2006.

[5] L. A. Chinitz and J. S. Sethi. How to perform noncontact mapping. *Heart Rhythm*, 3(1):120–123, 2006.

[6] S. J. Connolly. Atrial fibrillation in 2010: Advances in treatment and management. *Nature Reviews Cardiology*, 8:67–68, 2011.

[7] V. Fuster et al. ACC/AHA/ESC 2006 guidelines for the management of patients with atrial fibrillation–executive summary. *Circulation*, 114(7):700–752, 2006.

[8] S. Gojraty, N. Lavi, E. Valles, S. J. Kim, J. Michele, and E. P. Gerstenfeld. Dominant frequency mapping of atrial fibrillation: Comparison of contact and noncontact approaches. *Journal of Cardiovascular Electrophysiology*, 20(9):997–1004, 2009.

[9] C. C. Gornick, S. W. Adler, B. Pederson, J. Hauck, J. Budd, and J. Schweitzer. Validation of a new noncontact catheter system for electroanatomic mapping of left ventricular endocardium. *Circulation*, 99(6):829–835, 1999.

[10] P. Jais, M. Haissaguerre, D. C. Shah, S. Chouairi, L. Gencel, M. Hocini, and J. Clementy. A focal source of atrial fibrillation treated by discrete radiofrequency ablation. *Circulation*, 95(3):572–576, 1997.

[11] A. Kadish, J. Hauck, B. Pederson, G. Beatty, and C. Gornick. Mapping of atrial activation with a noncontact, multielectrode catheter in dogs. *Circulation*, 99(14):1906–1913, 1999.

[12] K. Kumagai, H. Nakashima, et al. Noncontact mapping-guided catheter ablation of atrial fibrillation. *Circulation*, 73(2):233–241, 2009.

[13] G. R. Mines. On dynamic equilibrium in the heart. *The Journal of Physiology*, 46(4-5):349–383, 1913.

[14] W. B. Nicolson, G. P. McCann, P. D. Brown, A. J. Sandilands, P. J. Stafford, F. S. Schlindwein, N. J. Samani, and G. A. Ng. A novel surface electrocardiogram–based marker of ventricular arrhythmia risk in patients with ischemic cardiomyopathy. *Journal of the American Heart Association*, 1(4), 2012.

[15] J. Salinet Jr, A. Ahmad, P. Brown, P. Stafford, A. Ng, and F. Schlindwein. Three-dimensional Frequency Mapping from the Noncontact Unipolar Electrograms in Atrial Fibrillation. In A. Murray, editor, *Computers in Cardiology, Belfast, Nothern Ireland, U.K.*, volume 37, pages 745–748, 2010.

[16] J. Salinet Jr, J. Ahuja, P. Brown, P. Stafford, A. Ng, and F. Schlindwein. Trajectory propagation of dominant frequency areas using high density noncontact mapping reveals distinct behaviour in persistent atrial fibrillation. In *Heart Rhythm 2012*, volume 9 of *May 2012 supplement*, pages S4–S5, 2012.

[17] J. Salinet Jr, P. Brown, A. Ahmad, J. Tuan, P. Stafford, A. Ng, and F. Schlindwein. High density noncontact frequency mapping reveals distinct dominant frequency behaviour in persistent atrial fibrillation. In *Heart Rhythm 2011*, volume 9 of *May 2012 supplement*, pages S4–S5, 2011.

[18] J. Salinet Jr, J. Madeiro, P. Cortez, P. Stafford, A. Ng, and F. Schlindwein. Removing ventricular influence from intracardiac atrial fibrillation electrograms. In *XXIII Congresso Brasileiro de Engenharia Biomédica - XXIII CBEB*, pages 1984–1988, 2012.

[19] R. J. Schilling, N. S. Peters, and D. W. Davies. Simultaneous endocardial mapping in the human left ventricle using a noncontact catheter. *Circulation*, 98(9):887–898, 1998.

[20] C.-T. Tai and S.-A. Chen. Noncontact mapping of the heart: How and when to use. *Journal of Cardiovascular Electrophysiology*, 20(1):123–126, 2009.